Transactions on the Built Environment vol 56, © 2001 WIT Press, www.witpress.com, ISSN 1743-3509

Suppression and characteristics of flow-induced vibration of rectangular prisms with various width-to-height ratios

H. Sakamoto, K. Takai, M. M. Alam and M. Moriya
Department of Mechanical Engineering, Kitami Institute of Technology, 165 Koen-Cho, Kitami, Hokkaido, 090-8507, Japan

Abstract

In this study, the response characteristics and suppression of flow-induced vibrations of rectangular prisms with various width-to-height ratios were experimentally investigated. The present study focused on rotary oscillation, one of the three types of flow-induced vibration generated in a rectangular prism. The main findings were that (i) there are three types of flow-induced vibration, i.e., vortex excitation, low-speed and high-speed torsional flutter, (ii) the flow-induced vibration occurs due to change in fluctuating pressure on the surface of the prism based on the difference of rolling-up of the shear layer separating from the leading edge of the prism, (iii) the flow-induced vibration can be classified into five patterns depending on the width-to-height ratio, and (iv) the flow-induced vibrations can be most effectively suppressed by placing a normal plate upstream of the prism.

1 Introduction

Flow-induced vibrations are major problems in various areas of engineering. Many studies on flow-induced vibrations have been made on circular cylinders and retangular prisms as representative structures. There have been several studies on response characteristics, generation mechanism and suppression of flow-induced vibrations of a rectangular prism [1]~[4]. However, there are still many unresolved issues, including the mechanism by which flow-induced vibration is generated, particularly in the case of a rectangular prism.

Flow-induced vibrations generated in a rectangular prism include cross-flow vibration (vibration of the prism in the direction normal to the flow), in-line vibration (vibration of the prism in the stream-wise direction), and rotary oscillation (oscillation of the prism with an angular displacement). The present study focused on the rotary oscillation type of flow-induced vibration. The response characteristics on elastically supported prisms were first examined in detail by free-vibration tests. Next, flow-induced vibrations obtained by the free-vibration tests were reproduced by forced-vibration tests, and the aerodynamic characteristics of the prisms, the behavior of the shear layer that separated from the leading edge, and the characteristics of the impinging leading-edge vortex, and the wake vortex were examined. The mechanism by which flow-induced vibrations are generated was examined on the basis of these results. Furthermore, the response characteristics in the case in which a normal plate was centrally placed upstream of the prism and in the case in which a splitter plate was placed downstream of the prism in order to suppress flow-induced vibrations were examined. The optimum method for suppressing flow-induced vibration of a rectangular prism was established on the basis of the results.

2 Experimental Setups and Procedures

Both free-vibration and forced-vibration tests were performed in the present study. In the forced-vibration tests, the characteristics of fluctuating pressure and aerodynamic forces acting on a rectangular prism were investigated by using a low-speed Eiffel-type wind tunnel. The test section of the wind tunnel was rectangular in shape with a height of 1.0 m, a width of 0.35 m, and a length of 2.0 m. The prism used in the forced-vibration tests had various widths but were all 100 mm in height. A semiconductor pressure transducer was installed inside for the measurement of fluctuating pressure on the upstream, downstream and side surfaces of the prism, as shown in Fig. 1. The aerodynamic forces were estimated from the ensemble-averaged fluctuating pressures. The prism was forced into rotary oscillation at an angular displacement of $\pm 5^\circ$. In the tests, the reduced velocity U_r [$=U/(f_c \cdot H)$, where U is the free-stream velocity, H is the height of the prism, and f_c is the natural frequency of the prism] was varied from 2.5 to 50. The

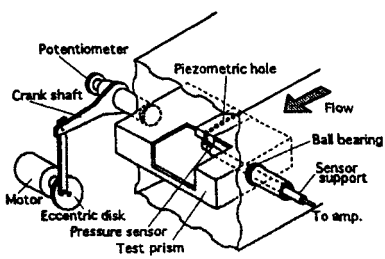

Figure 1: View of forced-vibration experimental setup.

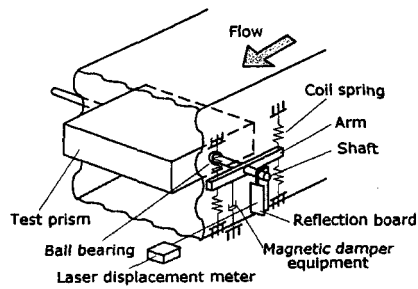

Figure 2: View of free-vibration experimental setup.

corresponding Reynolds number Re ($=UH/\nu$) was 2.65×10^4 to 7.28×10^4.

The free-vibration tests were carried out in a low-speed, closed-circuit wind tunnel. The test section of the wind tunnel was rectangular in shape with a width of 0.3 m, a height of 1.2 m, and a length of 2.5 m. The width-to-height ratio of the tested prism was changed from 0.3 to 6.0. The height of the prism used in each test was 100 mm. The prism was supported by four coil springs attached to the outside of the wind tunnel, as shown in Fig. 2, enabling rotary oscillation of the prism. Also, the reduced mass-damping factor Cn ($=I\delta/\rho B^4$, where I is the inertia moment per unit length of prism, δ is the logarithmic decrement of damping, and ρ is the density of fluid) was changed using two magnetic dampers. The response characteristics of rotary oscillation of the prism were investigated by varying the reduced velocity U_r from 1 to 35 for the plain prism and the controlled prism. The flow-induced vibration was suppressed by the use of a normal plate and a splitter plate placed upstream and downstream of the prism, respectively, as shown in Fig. 3. The angular displacement and oscillation frequency of the prism were measured using a laser-displacement meter. Also, flow patterns in a recirculating water channel with a test section of 30 cm in width, 40 cm in depth and 2 m in length were observed by uranine dye, which was injected from two holes, each with a diameter of 1 mm, located at upper and lower side in the neighborhood of the leading edge of the prism. Flow patterns generated at a constant free-stream velocity of U=0.8 cm/s were observed. The corresponding Reynolds number was 350.

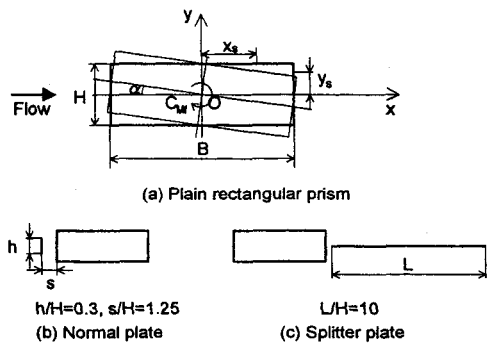

Figure 3: Coordinate system and definition of symbols.

3 Results and Discussion

3.1 Response characteristics of rotary oscillation of a rectangular prism

The flow-induced vibration generated in the rectangular prism differed with change in the width-to-height ratio of B/H. Figure 4 shows the response characteristics of rotary oscillation of the prism at each width-to-height ratio. The ordinate axis shows the rms value of angular displacement α of rotational oscillation, and the abscissa shows the reduced velocity U_r. The flow-induced vibrations generated are classified into the following five patterns. Namely, pattern 1 is generated only

vortex excitation with the limited vibration when *B/H* is smaller than 1.1. Pattern 2 is one in which the generated vortex excitation becomes divergent, in the range of *B/H* from 1.2 to 1.6. Pattern 3 is one in which there exists two types of flow-induced vibration, i.e., vortex excitation and high-speed torsional flutter, in the range of *B/H* from 1.7 to 2.6. The high-speed torsional flutter becomes divergent. Pattern 4 is one in which there exists three types of the flow-induced vibration, i.e., low-speed torsional flutter, vortex excitation and high-speed torsional flutter, in the range of *B/H* from 2.7 to 3.5. The low-speed torsional flutter with the limited vibration is generated by impinging leading-edge vortices formed on the side surface of the prism. Only the high-speed torsional flutter becomes divergent. Pattern 5 is one in which two types of flow-induced vibration, i.e., low-speed and

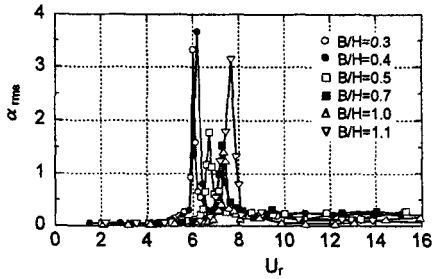

(a) *B/H* = 0.3 ~ 1.1 (Pattern 1)

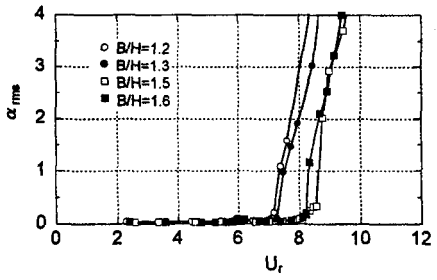

(b) *B/H* = 1.2 ~ 1.6 (Pattern 2)

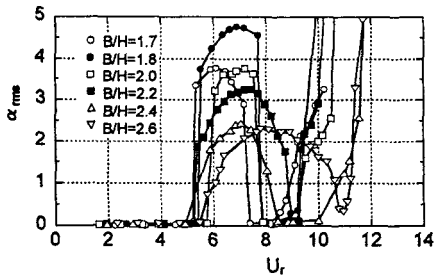

(c) *B/H* = 1.7 ~ 2.6 (Pattern 3)

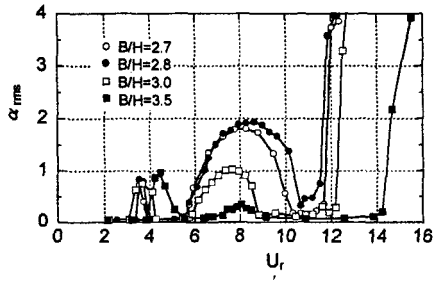

(d) *B/H* = 2.7 ~ 3.5 (Pattern 4)

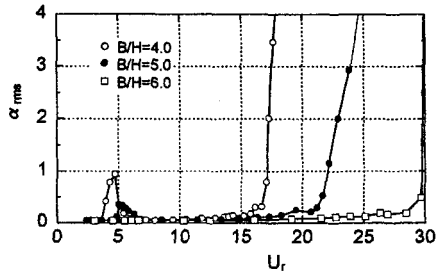

(e) *B/H* = 4.0 ~ 6.0 (Pattern 5)

Figure 4: Response characteristics of a rectangular prism with rotary oscillation.

high-speed torsional flutter, are generated when B/H exceeds 4.0. The high-speed torsional flutter becomes divergent.

3.2 Generation mechanism of flow-induced vibration

Figure 5 shows the distributions of fluctuating pressure on the surfaces in one cycle of rotary oscillation in the case of prisms with B/H ratios of 1.0 and 3.0 when vortex excitation occurs. The behavior of the shear layer separating from the leading edge of the prism is also shown in the figure. In the case of a rectangular

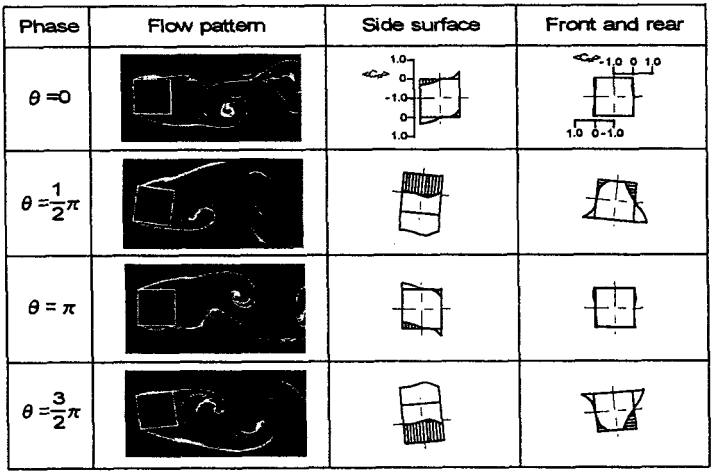

(a) $B/H = 1.0$ ($U_r = 7.6$)

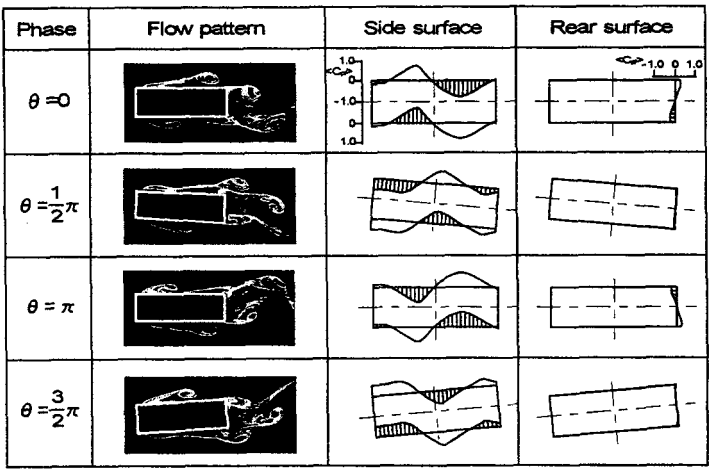

(b) $B/H = 3.0$ ($U_r = 7.0$)

Figure 5: Fluctuating pressure on the surfaces of prism and behavior of separated shear layer when vortex excitation occurs.

prism with *B/H* of 1.0, in which only vortex excitation occurs, fluctuating pressure is generated on the front, side and rear surfaces according to rolling-up of the shear layer separating from the leading edge of the prism. Because generating fluctuating pressure is asymmetric for the x- and y-axes, the fluctuating moment induced the rotary oscillation arises. In the case of a prism with *B/H* of 3.0, the shear layer separating from the leading edge rolls up alternately and attaches to the side surface. Due to the alternating rolling up of the shear layer, fluctuating pressure on the surface is generated. As a result, fluctuating pressure is asymmetric for the x- and y-axes and rotary oscillation therefore occurs.

Figure 6 shows the fluctuating pressure on the side and rear surfaces and the visualized flow pattern of the prism with *B/H* of 3.0 when low-speed and high-speed torsional flutter occur. In low-speed torsional flutter, impinging leading-edge vortices are formed on the side surface of the prism, and the position where the fluctuating pressure is negative corresponds to that of the impinging leading-edge vortex. Fluctuating pressure is generated due to downward movement of the impinging leading-edge vortices along the side surface. Therefore, it can be concluded that low-speed torsional flutter is induced by impinging leading-edge vortices formed on the side surface. In high-speed torsional flutter, the shear layer separating from the leading edge is rolled up without forming impinging leading-edge vortices. By the alternating rolling-up of the shear layer, large fluctuating pressure on the surface of the prism is generated, and high-speed torsional flutter is therefore induced.

Three types of flow-induced vibration, i.e., vortex excitation, low-speed torsional flutter and high-speed torsional flutter, are generated in the prism. It can be described by the work done fluid forces whether these flow-induced vibrations converge or diverge. The work W done fluid forces for one cycle of rotary oscillation is estimated by fluctuating moment C_{Mf} and angular displacement α as follows:

$$W = \int_{-\alpha}^{\alpha} C_{Mf}(\theta) \cdot d\alpha \,. \tag{1}$$

The fluctuating moment $C_{Mf}(\theta)$ in equation (1) is estimated by the following equation:

$$C_{Mf}(\theta) = \frac{1}{B^2} \int_{-B/2}^{B/2} \left\{ \left[< C_{pf}(\theta, x_s) > \cdot x_s \right]_{Upper} + \left[< C_{pf}(\theta, x_s) > \cdot x_s \right]_{Lower} \right\} dx$$

$$+ \frac{1}{H^2} \int_{-H/2}^{H/2} \left\{ \left[< C_{pf}(\theta, y_s) > \cdot y_s \right]_{Front} + \left[< C_{pf}(\theta, y_s) > \cdot y_s \right]_{Rear} \right\} dy \,, \tag{2}$$

where, $<C_{pf}>$ [$=1/N \cdot \Sigma\, p_f/(0.5\,\rho\, U^2)$, N: the ensemble-averaged number] is the ensemble-averaged fluctuating pressure coefficient, x_s and y_s are positions of the surface, and θ is each phase which is divided one cycle of the oscillation by number of partitions.

Figure 7 (a) and (b) show the values of work W estimated by equation (1) for

prism with *B/H* ratios of 1.0 and 3.0, respectively. In the prism with *B/H* of 1.0, *W* becomes positive (exciting force) in a limited narrow region where vortex excitation occurs. However, since *W* immediately becomes negative (damping force) as U_r increases, the vortex excitation may attenuate without diverging. In the prism with *B/H* of 3.0, *W* in the region in which vortex excitation and low-speed torsional flutter occurred becomes negative so that these become to be converged. On the other hand, *W* in the region in which high-speed torsional flutter occurred becomes positive over the whole range of values of U_r. The vibration becomes divergent without converging.

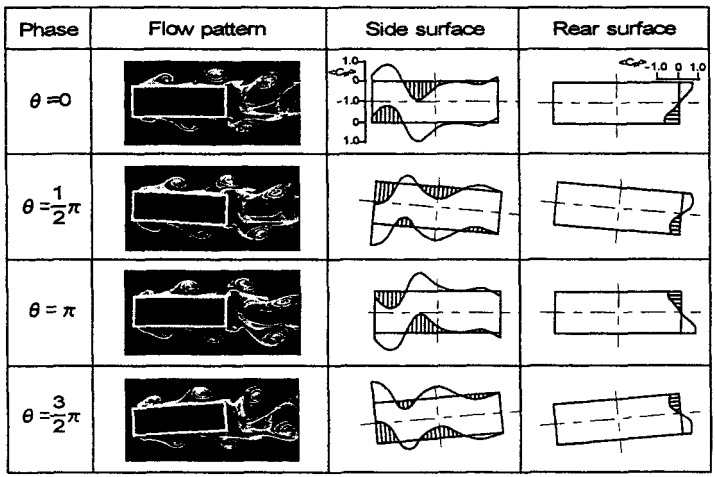

(a) Low-speed torsional flutter $B/H = 3.0$ ($U_r = 3.8$)

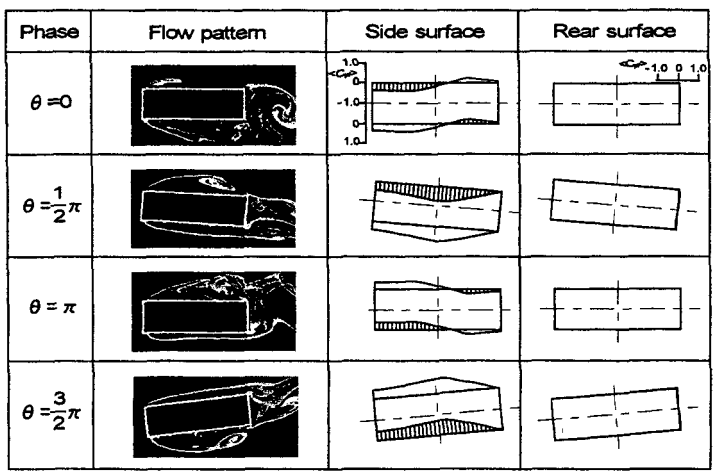

(b) High-speed torsional flutter $B/H = 3.0$ ($U_r = 29.0$)

Figure 6: Fluctuating pressure on the surfaces of prism and behavior of separated shear layer when low-speed and high-speed torsional flutter occur.

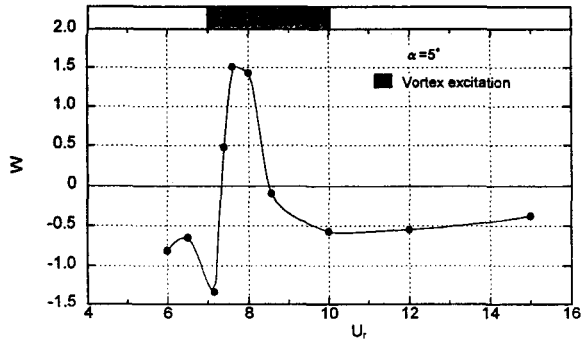

(a) Rectangular prism with B/H=1.0 occurred vortex excitation.

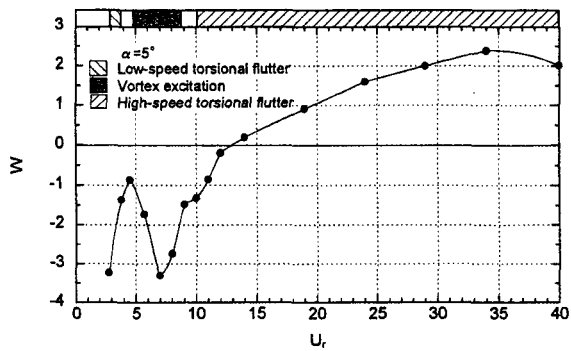

(b) Rectangular prism with B/H=3.0 occurred low-speed and high-speed torsional flutter and vortex excitation.

Figure 7: Work done by fluctuating moment versus U_r.

3.3 Suppression of flow-induced vibration

Figure 8 shows the response characteristics of flow-induced vibration when a normal plate with a width of 30 mm (h/H=0.3) is placed upstream of the prism (s/H=1.25). The low-speed and high-speed torsional flutters are completely suppressed because rolling-up of the shear layer that has separated from the leading edge of the prism is suppressed. However, because the shear layer that has separated from the leading edge attaches to the side surface and then rolls up again at the rear edge of the prism, a Karman vortex is formed when B/H is larger than 2.0. As a result, only vortex excitation with limited vibration is generated. Also, figure 8 shows the response characteristics of flow-induced vibration when a splitter plate with a length of L/H=10 is placed downstream of the prism. Because the formation of a Karman vortex is suppressed by the splitter plate, vortex excitation does not occur. However, low-speed and high-speed torsional flutters are generated.

As above mentioned, a normal plate placed upstream of the prism is very

effective for suppressing low-speed and high-speed torsional flutters. However, as shown in Fig. 8, vortex excitation occurs, while there is the weakness. Since the generated vortex excitation is limited vibration, it can be suppressed by increasing the reduced mass-damping factor *Cn*. Figure 9 shows the required values of *Cn* to suppress vortex excitation. Therefore, it becomes that vortex excitation can be completely suppressed by using values of *Cn* determined by the following equation (Eq. (3)).

$$\begin{aligned} Cn &= 0.325 \times (B/H)^{-2.50} && (B/H < 2.0) \\ Cn &= 0.419 \times (B/H)^{-1.03} && (B/H \geqq 2.0) \end{aligned} \tag{3}$$

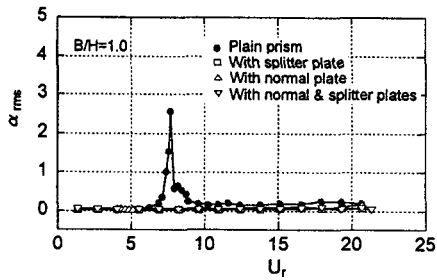

(a) $B/H = 1.0$ (Pattern 1)

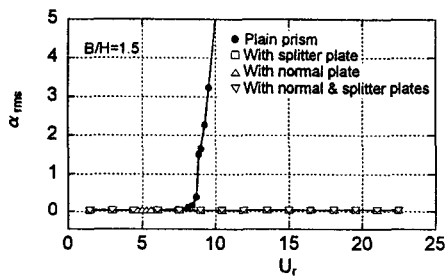

(b) $B/H = 1.5$ (Pattern 2)

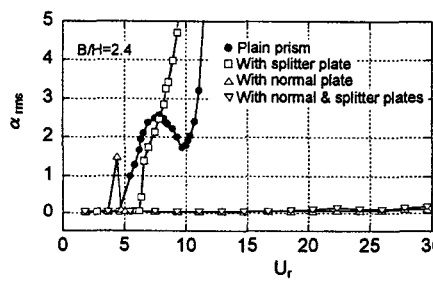

(c) $B/H = 2.4$ (Pattern 3)

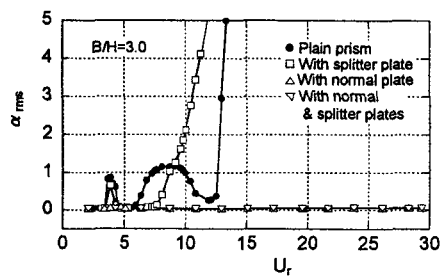

(d) $B/H = 3.0$ (Pattern 4)

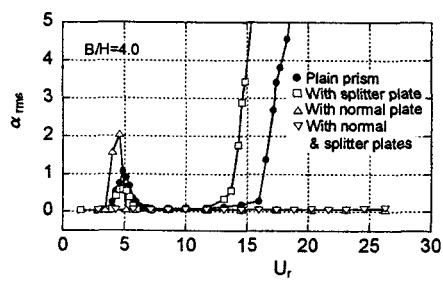

(e) $B/H = 4.0$ (Pattern 5)

Figure 8: Response characteristics of rectangular prism controlled using a normal plate and a splitter plate.

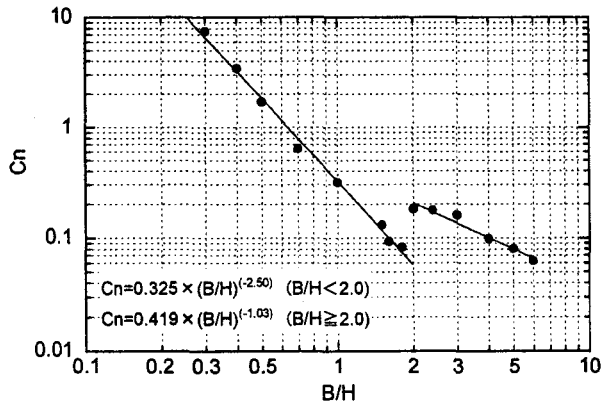

Figure 9: Required *Cn* suppressed vortex excitation when a normal plate is placed.

4 Concluding Remarks

(1) The results of free-vibration tests on plain rectangular prism showed that there are three types of flow-induced vibration, i.e., low-speed torsional flutter, vortex excitation and high-speed torsional flutter.
(2) Observation of the behavior of the shear layer separating from the leading edge of the prism indicated that flow-induced vibration occurs due to change in fluctuating pressure on the surface of the prism.
(3) Whether the generating flow-induced vibration becomes divergent or convergent can be described by the work done the fluid forces.
(4) A normal plate placed upstream of the rectangular prism can suppress the generation of low-speed and high-speed torsional flutters, and a splitter plate placed downstream of the rectangular prism can suppress the generation of vortex excitation.
(5) The generation of vortex excitation can be perfectly suppressed by increasing from the threshold value of for *Cn* when a normal plate is installed at the upstream of the prism.

References

[1] Naudascher, E. & Wang, Y. Flow-Induced Vibrations of Prismatic Bodies and Grids of Prisms. *J. Fluids and Struct.*, **7**, pp.341-373, 1993.
[2] Nakamura, Y. & Nakashima, M. Vortex excitation of prisms with elongated rectangular, H and ⊢ cross-sections. *J. Fluid Mech.*, **163**, pp.149-169, 1986.
[3] Shiraishi, N. & Matsumoto, M. On Classification of Vortex-induced Oscillation and its Application for Bridge Structures. *J. Wind Eng. and Ind. Aerodyn.*, **14**, pp.419-430, 1983.
[4] Komatsu, S. & Kobayashi, H. Vortex-Induced Oscillation of Bluff Cylinders. *J. Wind Eng. and Ind. Aerodyn.*, **6**, pp.335-362, 1980.